Journal of Molecular Structure 1118 (2016) 91–97

Contents lists available at ScienceDirect

Journal of Molecular Structure

journal homepage: http://www.elsevier.com/locate/molstruc

Novel amide-type ligand bearing bis-pyridine cores: Synthesis, spectral characterizations and X-ray structure analyses

Shaoyong Ke

National Biopesticide Engineering Research Center, Hubei Biopesticide Engineering Research Center, Hubei Academy of Agricultural Sciences, Wuhan, 430064, People's Republic of China

ARTICLE INFO

Article history:
Received 14 February 2016
Received in revised form
5 April 2016
Accepted 5 April 2016
Available online 7 April 2016

Keywords:
Amide
Ligand
Synthesis
Spectral characterizations
Crystal structure

ABSTRACT

The novel salicylamide-type ligand containing bis-pyridine moieties, i.e. 2-((6-chloropyridin-3-yl) methoxy)-*N*-(2-((6-chloropyridin-3-yl)methylthio)phenyl)benzamide, which has been successfully synthesized and characterized by typical spectroscopic techniques mainly including IR, ^{1}H NMR and ESI-MS. The structure of target compound was further determined by single crystal X-ray diffraction method and which crystallized in the monoclinic system with space group *P*2(1)/c.

1. Introduction

Carboxamide scaffolds have been known for a few decades, which attracted great attention as versatile ligands in numerous applications. Many carboxamide derivatives have been widely used in the field of coordination chemistry, and most of which can interact with various biologically important ions [1–4]. Meanwhile, many synthetic carboxamides have also been applied in material chemistry, and the broad biological activities of carboxamide-type derivatives have also been known for a long time [5–15]. Nowadays, many carboxamides derivatives have been developed as commercial medicines (such as BMS-354825, Finasteride, Dutasteride, and Lacosamide) and agrochemicals (such as Flonicamid, Tolfenpyrad, Chlorantraniliprole, Cyantraniliprole, Niclosamide, Penthiopyrad, Isotianil, Tiadinil, Mandipropamid, Mefenacet, and Propisochlor) (Fig. 1), and so which have played significantly important role in drug design and agrochemical industry.

Among these carboxamide skeletons, especially those multi-substituted salicylamide skeletons arouse many researchers' interest, which have been demonstrated to be important structural unit with diverse use in various biochemical process and coordination chemistry [16]. Up to now, many salicylamide derivatives have been demonstrated to present widely medicinal activities such as EGFR PTK inhibitors [17], antiviral activity [18], anti-tuberculosis activity [19], antibacterial activity [20], anti-inflammatory activities [21], antimycobacterial activity [22], cercaricidal activity [23], and aldose reductase inhibitors [24].

Thus, there is a great demand for the development of novel synthetic ligands capable of selective interaction with biomolecules or biologically important ions. In the present study, we focus on the synthesis and characterization of neotype salicylamide ligand bearing bis-pyridine moieties as shown in Scheme 1. Its structure was confirmed by typical spectroscopic methods mainly including IR, ^{1}H NMR, ESI-MS spectra, and single crystal X-Ray diffraction structural analysis has also been applied for further study on its detail structural information.

2. Experimental

2.1. Materials and general methods

All melting points (m.p.) were obtained using a digital model X-5 apparatus and are uncorrected. Infrared (IR) spectra in potassium bromide (KBr) were recorded on a Thermo Nicolet FT-IR Avatar 330 instrument. ^{1}H NMR spectra were recorded on a Bruker spectrometer at 600 MHz with $CDCl_3$ as the solvent and TMS as the internal standard. Chemical shifts are reported in δ (parts per

E-mail addresses: keshaoyong@163.com, shaoyong.ke@nberc.com.

http://dx.doi.org/10.1016/j.molstruc.2016.04.012
0022-2860/

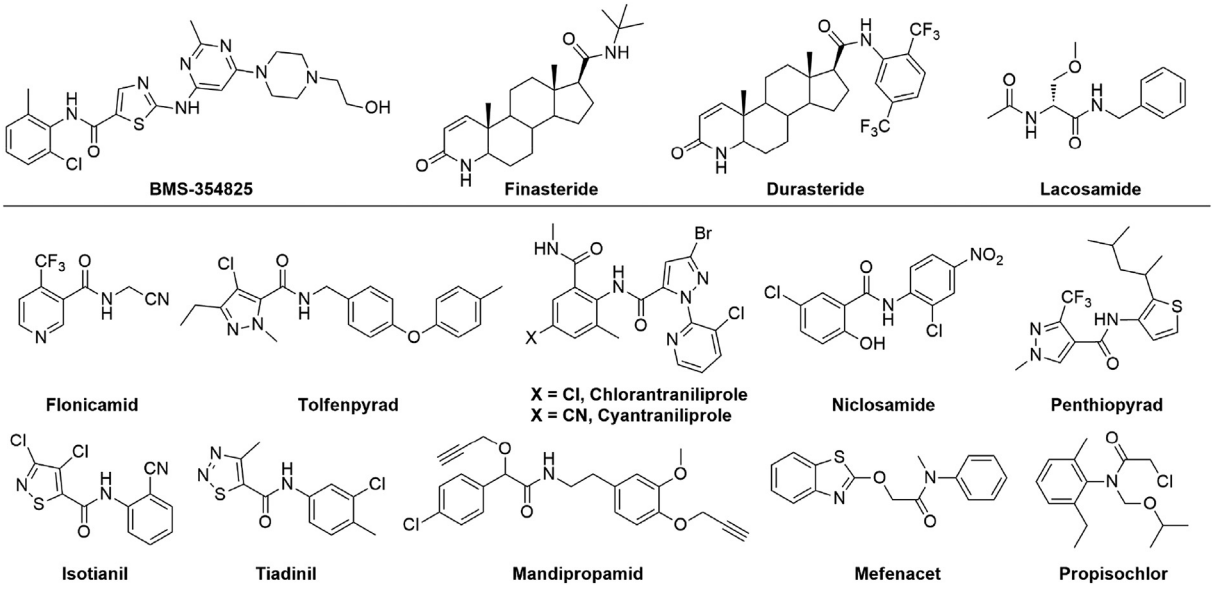

Fig. 1. Representative structure of drugs and pesticides containing amide units.

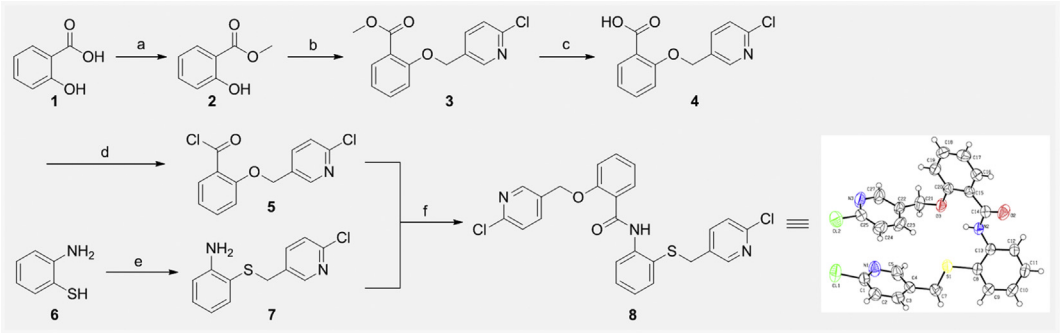

Scheme 1. Reagents and conditions: a. MeOH, Conc. H_2SO_4; b. 2-Chloro-5-(chloromethyl)pyridine, K_2CO_3, MeCN, r.t. to reflux for 10–12 h; c. NaOH, methanol/H_2O, rt to 50 °C for 5–7 h; d. $SOCl_2$, reflux for 4–6 h; e. 2-Chloro-5-(chloromethyl)pyridine, K_2CO_3, MeCN, r.t.; f. Et_3N, DMAP, DCM, r.t. for 2–5 h.

million) values. Coupling constants ^nJ are reported in Hz. Mass spectra were performed on a WATERS ACQUITY UPLC® H-CLASS PDA (Waters®) instrument. Analytical thin-layer chromatography (TLC) was carried out on precoated plates, and spots were visualized with ultraviolet light. All chemicals or reagents used for syntheses were commercially available, were of AR grade, and were used as received. All anhydrous solvents were dried according to standard methods. All other solvents and reagents were analytical reagent and used directly without purification.

2.2. Syntheses of target molecule **8**

2.2.1. General synthetic procedure for 2-((6-chloropyridin-3-yl) methoxy)benzoic acid **4** and 2-((6-chloropyridin-3-yl)methoxy) benzoyl chloride **5**

The key intermediate 2-((6-chloropyridin-3-yl)methoxy)benzoic acid **4** and 2-((6-chloropyridin-3-yl)methoxy)benzoyl chloride **5** was routinely prepared via multi-steps according to document method [25,26].

2.2.2. General synthetic procedure for 2-((6-chloropyridin-3-yl) methylthio)aniline **7**

To a solution of 2-aminobenzenethiol (1.25 g, 10 mmol) and K_2CO_3 (1.52 g, 11 mmol) in MeCN (25 mL) was added 2-chloro-5-(chloromethyl)pyridine (1.62 g, 10 mmol). The resultant mixture was stirred at room temperature for sever hours, which was detected by TLC. Then the mixture was charged with water and extracted with ethyl acetate, the organic phase was separated and dried over anhydrous Na_2SO_4. After filtered and concentrated, the organic residue is purified by silica gel column-chromatography.

2.2.3. General synthetic procedure for the target compound **8**

The typical process of synthesis of novel salicylamide derivative containing 2-chloro-5-pyridyl moiety **8** is shown as following: The freshly formed acylchloride **5** (2.2 mmol) dissolved in dry dichloromethane was added dropwise to a solution of the substituted aniline **7** (2 mmol), Et_3N (2.5 mmol), and catalytic amount of DMAP in dry dichloromethane under ice-bath. The resultant solution was stirred at room temperature for 2–5 h, which was detected by TLC. Then the mixture was washed to neutral with water and dried via anhydrous Na_2SO_4. After filtered and concentrated, the organic residue is purified by silica gel column-chromatography (ethyl acetate/petroleum ether) or recrystallization to give white solid or crystal. Their physico–chemical properties and the spectra data are as follows: 2-((6-chloropyridin-3-yl)methoxy)-*N*-(2-((6-chloropyridin-3-yl)

Table 1
Crystal data and structure refinement for target compound **8**.

Parameter	Data
Empirical formula	$C_{25}H_{19}Cl_2N_3O_2S$
Formula weight	496.39
Crystal system	Monoclinic
Space group	*P*2(1)/c
Unit cell dimensions	$a = 15.1485(9)$ Å, $\alpha = 90°$ $b = 7.7630(5)$ Å, $\beta = 97.7130(10)°$ $c = 19.9163(12)$ Å, $\gamma = 90°$
Volume	2320.9(2) Å^3
Z, Density (calculated)	4, 1.421 Mg/m^3
Absorption coefficient	0.398 mm^{-1}
F(000)	1024
Crystal size	0.16 × 0.12 × 0.10 mm^3
Theta range for data collection	2.06–28.29°
Index ranges	$-20 \le h \le 20 - 10 \le k \le 10 - 26 \le l \le 26$
Reflections collected	27650
Independent reflections	5741 [*R*(int) = 0.0406]
Completeness to theta = 28.29°	99.4%
Max. and min. transmission	0.9613 and 0.9390
Refinement method	Full-matrix least-squares on F^2
Data/restraints/parameters	5741/0/301
Goodness-of-fit on F^2	1.143
Final *R* indices [$I > 2$sigma(I)]	$R1 = 0.0602$, $wR2 = 0.1518$
R indices (all data)	$R1 = 0.0659$, $wR2 = 0.1558$
Largest diff. peak and hole	0.333 and−0.250 e.Å^{-3}

methylthio)phenyl)benzamide: yellowish crystal, yield 83%, m.p. 112–114 °C; IR (ν_{max}, KBr, cm^{-1}): 3281.77, 1662.75, 1586.26, 1574.49, 1562.71, 1526.43, 1457.74, 1197.71, 1009.32, 820.93, 758.95, 747.34; ^{1}H NMR (600 MHz, $CDCl_3$) δ 10.44 (s, 1H, NH), 8.57 (d, $J = 7.2$ Hz, 1H, Py–H), 8.46 (s, 1H, Py–H), 8.26 (d, $J = 7.8$ Hz, 1H, Py–H), 8.01 (s, 1H, Py–H), 7.70 (d, $J = 8.4$ Hz, 1H, Py–H), 7.50–7.00 (m, 9H, Py–H and Ph-H), 5.34 (s, 2H, OCH_2), 3.73 (s, 2H, SCH_2); ESI-MS: *m*/*z* 496.3 $(M + H)^+$, 518.2 $(M + Na)^+$, calcd for $C_{25}H_{19}Cl_2N_3O_2S$ *m*/*z* = 495.1.

2.3. X-ray crystallography

Crystals of target molecule **8** suitable for X-ray crystal structure determination was obtained from a mixed solution of acetone and alcohol. The resultant crystals were separated from the solution by decanting. Yellowish crystal of **8** (0.16 mm × 0.12 mm × 0.10 mm) were counted on a quartz fiber with protection oil. Cell dimensions and intensities were measured at 298 K on a Bruker SMART CCD area detector diffractometer with graphite monochromated Mo Kα radiation ($\lambda = 0.71073$ Å); $\theta_{max} = 28.29$; 27,650 measured reflections; 5741 independent reflections ($R_{int} = 0.0406$). Data were corrected for Lorentz and polarization effects and for absorption ($T_{min} = 0.9390$; $T_{max} = 0.9613$). The structure was solved by direct methods using SHELXS-2001 [27]; all other calculations were performed with Bruker SAINT System and Bruker SMART programs

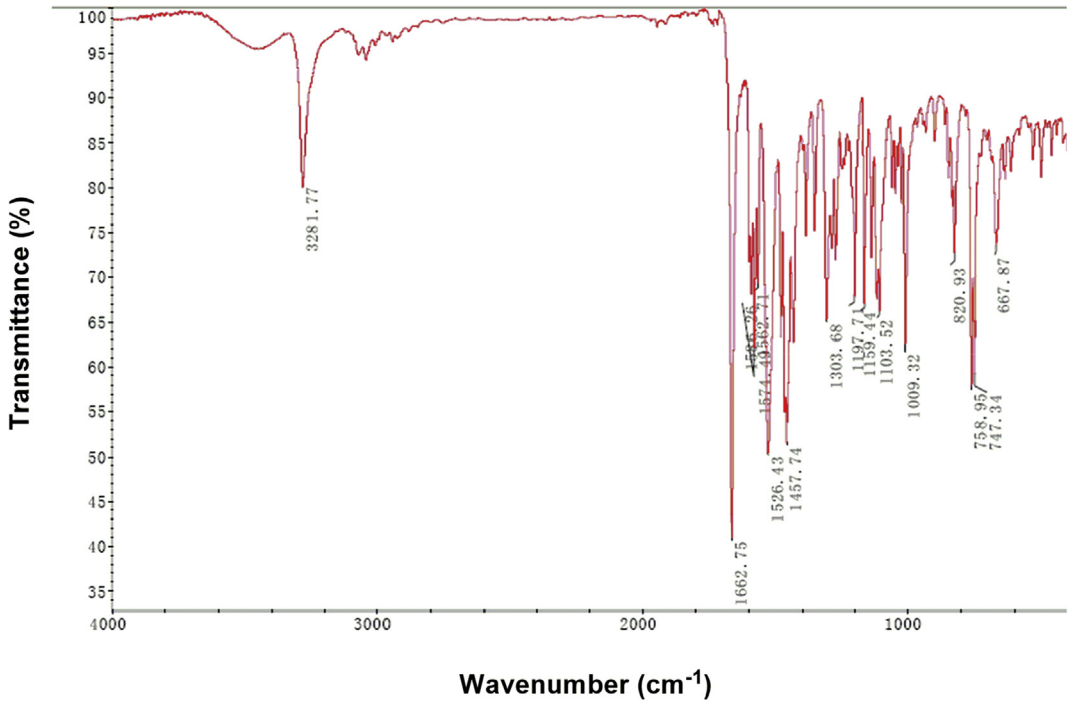

Fig. 2. The IR spectra analyses of compound **8**.

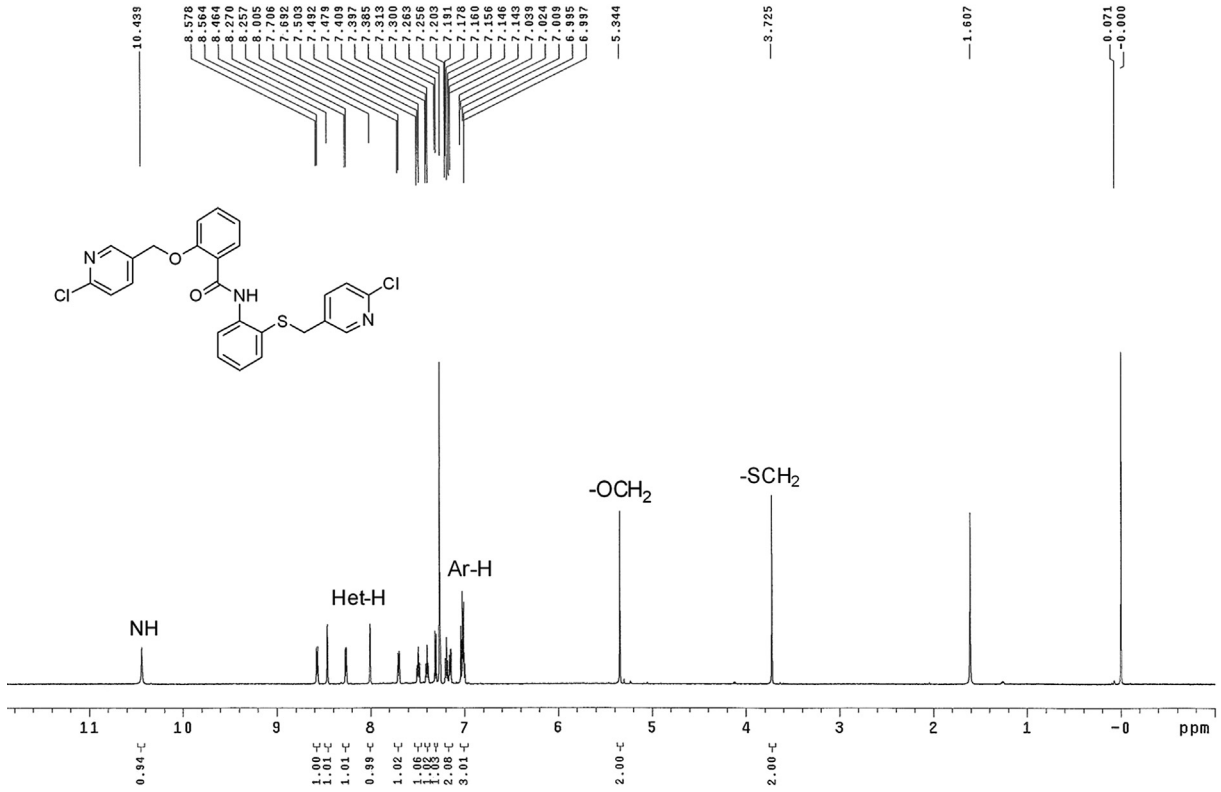

Fig. 3. The ^{1}H NMR spectra analyses of compound **8.**

[28]. Full-matrix least-squares refinement based on F^2 using the weight of $1/[\sigma^2(F_o^2) + (0.0849P)^2 + 0.0555P]$ gave final values of $R = 0.0602$, $\omega R = 0.1518$, and GOF(F) = 1.143. The fractional coordinates, all bond lengths and angles, and the anisotropic displacement parameters have been deposited as Supporting Information, and the crystallographic and refinement data of **8** is shown in Table 1.

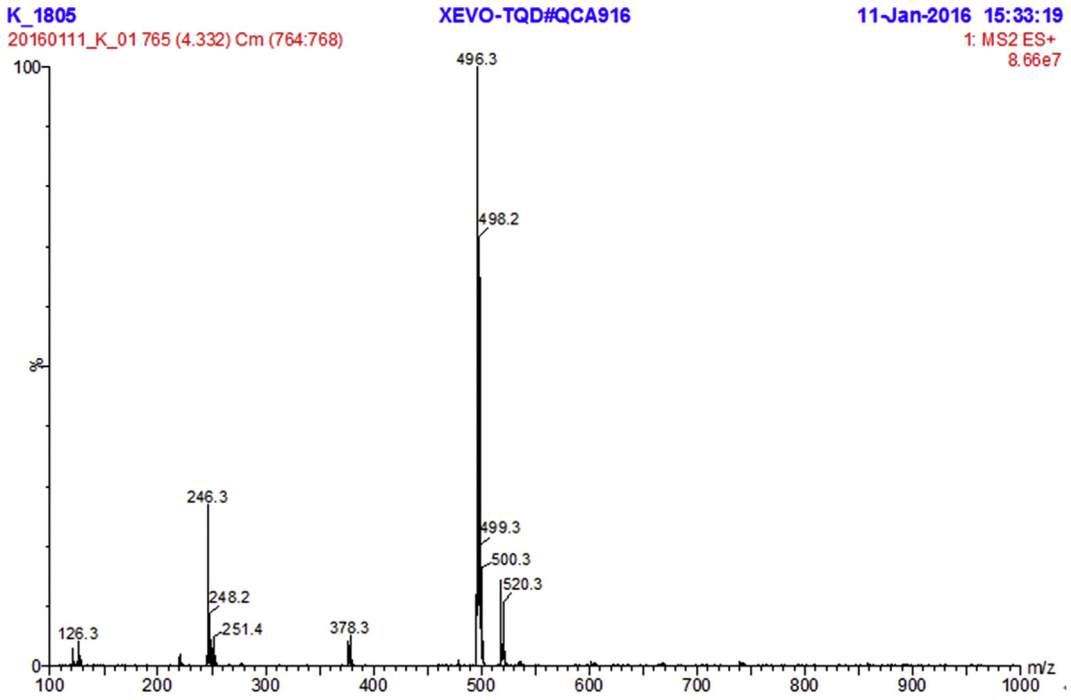

Fig. 4. The ESIMS spectra analyses of compound **8.**

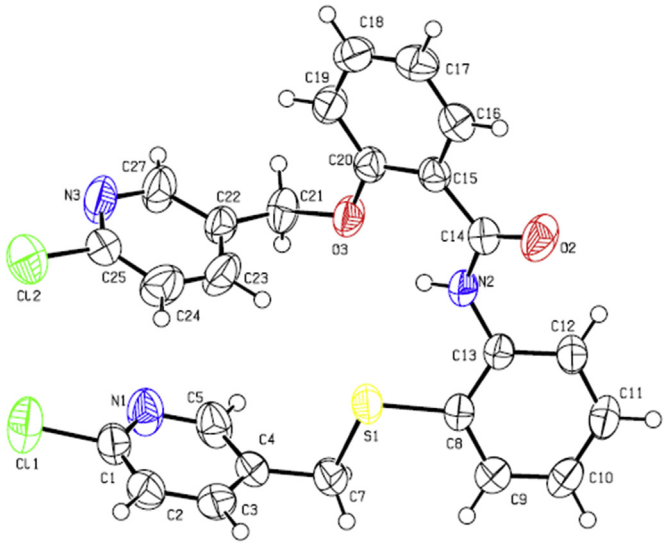

Fig. 5. The ORTEP diagram of **8**, showing the atom-labeling scheme. Displacement ellipsoids are drawn at the 50% probability level.

3. Results and discussion

3.1. Synthesis of salicylamide derivative containing bis-pyridine moieties

In the present study, a novel amide ligand derived from salicylic acid was synthesized by reacting functionalized salicylic acid with substituted-amine. The general methods for the preparation of target molecule containing bis-pyridine moieties **8** are outlined in Scheme 1.

The low-cost salicylic acid was selected as raw materials, which was routinely transferred to the corresponding intermediates **4** via three steps according to document method [25,26]. Activation of the substituted carboxylic acid **4** with thionyl chloride provides the corresponding acid chloride **5**, which was further used to couple with newly prepared amine **7** to give the ligand **8**. The target molecule **8** gave satisfactory chemical analyses, and all the IR, ^{1}H NMR, ESI-MS spectra were consistent with the assigned structure. Furthermore, the crystal of target molecule has been obtained by recrystallization method, and the single-crystal structure was determined by X-Ray diffraction.

3.2. Spectroscopic studies on compound *8*

The structure of target molecule **8** was confirmed by its IR, ^{1}H NMR spectra and electron spray impact mass spectra (ESI-MS) analyses. The IR spectra was measured with a Thermo Nicolet FT-IR Avatar 330 spectrophotometer using KBr pellets and shown in Fig. 2. As we can find that the IR spectra for target molecule showed obvious signals of NH, which presented a band at 3281.77 cm^{-1}. The obvious adsorption signal at 1662.75 cm^{-1} in the IR spectra of compound **8** was assigned to the carbonyl of amide as shown in the following spectra. For compound **8**, the bands that appeared in its IR spectra such as 1586.26, 1574.49, 1562.71, 1562.43 and 1457.74 cm^{-1} were attributed to the typical carbon–carbon stretching vibrations of heteroaromatic rings. The bands observed at 1197.71 and 1009.32 cm^{-1} in the IR spectrum are assigned to C–O bending vibration for title compound. The wavenumbers observed at 820.93, 758.95, and 747.34 cm^{-1} have been assigned to the typical aromatic ring vibrational modes.

The ^{1}H NMR spectra showed distinctive signals of methylene between oxygen/sulfur and pyridine ring, which presented a singlet at 5.34 and 3.73 ppm, respectively. The broad singlet at 10.44 ppm in the ^{1}H NMR spectra of compounds **8** was assigned to the NH proton of amide as shown in the representative spectra (Fig. 3). For compound **8**, the signals that appeared in its ^{1}H NMR spectra in the ranges 8.57–7.50 ppm were attributed to the typical protons of pyridine heterocycles.

The electron spray impact mass spectra (ESI-MS) for compound **8** was measured with a Mass spectra were performed on a WATERS ACQUITY UPLC® H-CLASS PDA (Waters®) instrument, and the ion peak or adduct ions of the synthesized compound were investigated as shown in Fig. 4. Experimentally, in the positive ion mode, the ESI-MS of compound **8** exhibit the obvious molecular peak $[M+H]^+$ appeared at *m*/*z* 496.8 with high abundance (100%), and the peak appears at *m*/*z* 518.2 was assigned to the corresponding sodium adduct ions (15–20%). The medium abundance peaks at *m*/*z* 246.3 presented in the ESI mass spectra were assigned to the cleavage fragments $[M-NHR]^+$. The lowest abundance peaks at *m*/*z* 126.3 were assigned to further cleavage fragments $[ClPyCH_2]^+$.

3.3. Crystal structure determination of compound *8*

In order to explore the possible molecule structure and hydrogen-bonding systems, the crystal structure of molecule **8** has also been studied. Compound **8** is crystallized in monoclinic crystal system with *P*2(1)/c space group, unit cells *a* = 15.1485(9) Å,

Table 3
Hydrogen bond geometry (Å,°).

D-H···A	d(D-H)	d(H···A)	d(D···A)	<(DHA)
N(2)–H(2A) ···O(3)	0.80(3)	1.92(3)	2.618(2)	145(3)
C(27)–H(27)···N(1)#1	0.93	2.43	3.347(3)	169.8

Symmetry transformations used to generate equivalent atoms: #1 -x + 1, y + 1/2, -z + 1/2.

Table 2
Selected bond lengths (Å), bond angles (°) and torsion angles (°) for compound **8**.

Bond lengths (Å)		Bond angles (°)		Torsion angles (°)	
C(1)–N(1)	1.307(3)	N(1)–C(1)–C(2)	124.7(2)	C(3)–C(4)–C(7)–S(1)	−91.5(2)
C(1)–C(2)	1.374(3)	N(1)–C(1)–Cl(1)	116.23(18)	C(5)–C(4)–C(7)–S(1)	83.9(3)
C(1)–Cl(1)	1.743(2)	N(1)–C(5)–C(4)	124.5(2)	C(4)–C(7)–S(1)–C(8)	178.40(16)
C(5)–N(1)	1.337(3)	N(1)–C(5)–H(5)	117.8	C(9)–C(8)–S(1)–C(7)	−21.4(2)
C(7)–S(1)	1.799(2)	O(3)–C(21)–C(22)	112.81(19)	C(8)–C(13)–N(2)–C(14)	145.3(2)
C(21)–O(3)	1.437(2)	O(3)–C(20)–C(15)	117.09(17)	C(12)–C(13)–N(2)–C(14)	−37.4(3)
C(20)–O(3)	1.371(3)	C(20)–O(3)–C(21)	120.49(17)	C(13)–C(8)–S(1)–C(7)	159.65(17)
C(8)–S(1)	1.7645(19)	S(1)–C(7)–H(7A)	110.9	C(15)–C(14)–N(2)–C(13)	−177.51(18)
C(14)–O(2)	1.213(2)	C(9)–C(8)–S(1)	123.74(17)	O(3)–C(21)–C(22)–C(23)	−35.8(3)
C(14)–N(2)	1.354(3)	C(8)–S(1)–C(7)	106.04(10)	O(3)–C(21)–C(22)–C(27)	145.8(2)
C(13)–N(2)	1.413(3)	O(2)–C(14)–N(2)	122.4(2)	C(15)–C(20)–O(3)–C(21)	179.17(19)

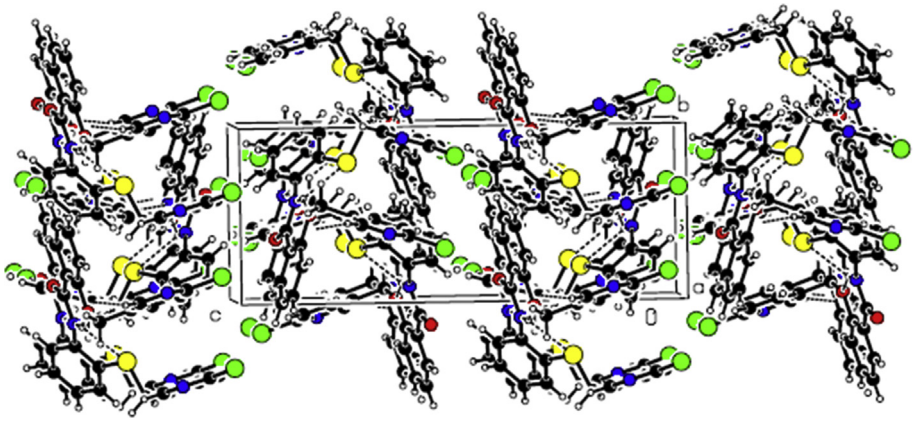

Fig. 6. Packing diagram of target compound **8**, and the dashed lines denote intermolecular hydrogen bonds.

$b = 7.7630(5)$ Å, $c = 19.9163(12)$ Å and $\beta = 97.7130(10)^\circ$. An Ortep view of the target compound is shown in Fig. 5, and the crystallographic and refinement data of **8** is listed in Table 1.

The title molecule can be described as being built from planar fragments, mainly including phenyl ring A (C8/C9/C10/C11/C12/C13), B (C15/C16/C17/C18/C19/C20), and pyridine ring C (C1/C2/C3/C4/C5/N1) and D (C22/C23/C24/C25/N3/C27) linking by −CONH−, $-OCH_2-$ and $-SCH_2-$ groups, respectively. The pyridine ring C and D are essentially parallel, however, the phenyl ring A and B are not parallel, and there exist an obvious dihedral angle (17.545°) between them. This is undoubtedly due to the hydrogen bong interaction from amide bond between these two phenyl rings. Meanwhile, the phenyl ring B and pyridine ring D is nearly perpendicular (88.944°), however, a dihedral angle (25.558°) exists between the phenyl ring A and pyridine ring C, which are a result of the different electron withdrawing effects of sulfur and oxygen atoms.

3.4. Intermolecular interactions and packing relations

The typical bond length and angles for compound **8** are presented in Table 2, and most of which are in good agreement with the reasonable range of standard values. The bond lengths C14−N2 (1.354(3)Å) are shorter than the normal C−N (1.472 Å) bond length because of the partial double bond character for amide bond. These can also be attributed to the presence of resonance in this fragment and forming a planar six-membered ring with N2−H2A···O3 hydrogen bond (Table 3). Furthermore, the bond angles for C(20)-O(3)-C(21) and C(8)-S(1)-C(7) are 120.49(17)° and 106.04(10)°, respectively, which are a result of the different steric effects of a lone-pair electron for sulfur and oxygen atoms.

There is an obvious intramolecular hydrogen bond, N2−H2A···O3 closing a pseudo-six-membered ring (O3···H2A−N2−C14−C15−C20−O3) (Table 3). In the crystal lattice, there are face-to-face π−π stacking interactions between the two phenyl rings from two molecules (Fig. 6), which leads to a layer framework along the *a*-axis. These hydrogen bonds and π−π stacking interactions play key roles in stabilizing the crystal packing.

4. Conclusion

In summary, we have described the synthesis, characterizations and structure analysis of a novel salicylamide-type ligand containing bis-pyridine group. This novel amide ligand has been conveniently synthesized, and fully characterized by IR, ^{1}H NMR, ESI-MS spectra. The further X-ray diffraction analyses demonstrated the target ligand exhibits monoclinic crystal system. To our best knowledge, this is the first investigate the structure features of pyridine-functional salicylamide ligand, which is promising potential compound for developing novel amide ligand for broad applications in the coordination chemistry. Further application and properties about the designed novel amide ligand are well ongoing in our laboratory.

Acknowledgment

This work was financially supported by the Projects from Hubei Agricultural Science Innovation Centre (2012-620-008-002, 2015-620-003-001) and the Key Laboratory of Integrated Pest Management in Crops in Central China, Ministry of Agriculture and Key Laboratory for Crop Diseases, Insect Pests and Weeds Control in Hubei Province (2015ZTSJJ9).

Appendix A. Supplementary data

Supplementary data related to this article can be found at http://dx.doi.org/10.1016/j.molstruc.2016.04.012.

References

[1] H.G. Lee, J.H. Lee, S.P. Jang, H.M. Park, S.-J. Kim, Y. Kim, C. Kim, R.G. Harrison, Tetrahedron 67 (2011) 8073–8078.
[2] Y. Zhang, X. Guo, L. Jia, S. Xu, Z. Xu, L. Zheng, X. Qian, Dalton Trans. 41 (2012) 11776–11782.
[3] L.H. Wu, L.F. Han, Y.B. Ruan, Y.B. Jiang, Chin. J. Anal. Chem. 38 (2010) 121–124.
[4] J. Zheng, Y. Chen, K. Wu, C. Ran, Y. Xu, M. Song, Chin. J. Org. Chem. 33 (2013) 1536–1539.
[5] B. Shen, D.M. Makley, J.N. Johnston, Nature 465 (2010) 1027–1033.
[6] J. Med. Chem. 47 (2004) 6658–6661.
[7] N. Pradidphol, N. Kongkathip, P. Sittikul, N. Boonyalai, B. Kongkathip, Eur. J. Med. Chem. 49 (2012) 253–270.
[8] F. Piscitell, A. Ligresti, G. La Regina, A. Coluccia, L. Morera, M. Allara, E. Novellino, V. Di Marzo, R. Silvestri, J. Med. Chem. 55 (2012) 5627–5631.
[9] T. Suzuki, M.N.A. Khan, H. Sawada, E. Imai, Y. Itoh, K. Yamatsuta, N. Tokuda, J. Takeuchi, T. Seko, H. Nakagawa, N. Miyata, J. Med. Chem. 55 (2012) 5760–5773.
[10] H. Rajak, P. Kumar, P. Parmar, B.S. Thakur, R. Veerasamy, P.C. Sharma, A.K. Sharma, A.K. Gupta, J.S. Dangi, Eur. J. Med. Chem. 53 (2012) 390–397.
[11] Z. Wang, B. Liu, Y. Li, W. Zhao, Chin. J. Org. Chem. 31 (2011) 317–323.
[12] T.C. Castral, A.P. Matos, J.L. Monteiro, F.M. Araujo, T.M. Bondancia, L.G. Batista-Pereira, J.B. Fernandes, P.C. Vieira, M.F.G.F. da Silva, A.G. Correa, J. Agric. Food Chem. 59 (2011) 4822–4827.
[13] H. Song, Y. Liu, L. Xiong, Y. Li, N. Yang, Q. Wang, J. Agric. Food Chem. 60 (2012) 1470–1479.
[14] Z. Wu, L. Zheng, Y. Li, F. Su, X. Yue, W. Tang, X. Ma, J. Nie, H. Li, Food Chem. 134 (2012) 1128–1131.
[15] Z. Fang, H. Jiang, X. Ye, Eur. J. Chem. 9 (2012) 211–218.
[16] L. Guo, Q. Wang, Q. Jiang, Q. Jiang, Y. Jiang, J. Org. Chem. 72 (2007) 9947–9953.

[17] S. Kamatb, J.K. Buolamwini, Med. Res. Rev. 26 (2006) 569–594.
[18] M. Krátký, J. Vinšová, Mini-Rev. Med. Chem. 11 (2011) 956–967.
[19] J.M. Férriz, K. Vávrová, F. Kunc, A. Imramovský, J. Stolaríková, E. Vavríková, J. Vinšová, Bioorg. Med. Chem. 18 (2010) 1054–1061.
[20] K. Cheng, Q. Zheng, Y. Qian, L. Shi, J. Zhao, H. Zhu, Bioorg. Med. Chem. 17 (2009) 7861–7871.
[21] M.E. Brown, J.N. Fitzner, T. Stevens, W. Chin, C.D. Wright, J.P. Boyce, Bioorg. Med. Chem. 16 (2008) 8760–8764.
[22] M. Krátký, J. Vinšová, N.G. Rodriguez, J. Stolaríková, Molecules 17 (2012) 492–503.
[23] W. Wang, Z. Qin, D. Zhu, Y. Wei, S. Li, L. Duan, Antimicrob. Agents Chemother. 60 (2016) 323–331.
[24] M.C. Van Zandt, E.O. Sibley, E.E. McCann, K.J. Combs, B. Flam, D.R. Sawicki, A. Sabetta, A. Carrington, J. Sredy, E. Howard, A. Mitschler, A.D. Podjarny, Bioorg. Med. Chem. 12 (2004) 5661–5675.
[25] S. Li, X. Cao, C. Chen, S. Ke, Spectrochim. Acta A 96 (2012) 18–23.
[26] S. Ke, Z. Zhang, T. Long, Y. Liang, Z. Yang, Med. Chem. Res. 22 (2013) 3621–3628.
[27] G.M. Sheldrick, SHELXTL (Version 5.0), University of GÖttingen, Göttingen, Germany, 2001.
[28] SMART V5.628, SAINT V6.45, and SADABS, Bruker AXS Inc., Madison, WI, 2001.